INTERACTION OF A POLYDISPERSED WATER MIST WITH A LAMINAR NON-PREMIXED JET FLAME

Sonny J. Lewis,[+] Jean-Pierre Delplanque,[*] Abhijit U. Modak,[+] and Robert J. Kee [+]
[+]Center for Commercial Applications of Combustion in Space
Division of Engineering
Colorado School of Mines
Golden, CO 80401

[*]Mechanical and Aeronautical Engineering
Center for Computational Science and Engineering
University of California, Davis
Davis, CA 95616
Ph: (530) 754-6950, E-mail: delplanque@ucdavis.edu

ABSTRACT

Numerical simulations of the interaction of a polydispersed water mist and a flame, with the specific goal of determining fire suppression characteristics, are very computation intensive. Even in geometrically simple configurations, such as co-flowing flames, the computational cost of a full Navier-Stokes solution of the reacting flow alone, without droplets, is very high. A boundary-layer approach is developed here which provides the needed efficiency; a typical non-premixed flame including chemical kinetics with hundreds of reactions and multicomponent transport is solved in a few minutes on a personal computer. This is compared to many hours or even days that are required to simulate the equivalent problems with full Navier-Stokes equations. This paper discusses the range of circumstances for which the boundary-layer approximations are valid. Preliminary results characterizing the one-way coupled interaction of a water mist with a laminar non-premixed flame are also presented.

INTRODUCTION

Water-mist offers an efficient, environmentally benign alternative to halon fire suppression agents. Investigations of the fire-suppression characteristics of water-mist, whether experimental or numerical, naturally span the wide range of relevant scales, from fires in full-scale compartments and lockers [1–4] to the microscale interaction between mist droplets and model flames [5–8]. Because of their reduced dimensionality, the latter allow the consideration of detailed chemistry and provide valuable insight that cannot be obtained in large-scale studies. For instance, the opposed-flow configuration lends itself to computational modeling of non-premixed flames in a one-dimensional setting via mathematical similarity. Consequently very large reaction mechanisms can be incorporated in the modeling with modest computational cost. Understanding flame structure from a chemical-kinetics viewpoint usually requires varying reaction mechanisms and parameters, seeking agreement between models and experimental observation. Beyond the direct relevance to the suppression and extinction of flames with fine water mist mentioned above, there are many other applications that need increased attention to

chemical details. For example, these may include the destruction of toxic-waste streams or the flame synthesis of oxide nano-particles.

Another non-premixed flame laboratory configuration that finds widespread utility is that of a jet of fuel issuing in a co-flowing oxidizer stream, as illustrated in Fig. 1. Unlike the opposed-flow situation, the jet flame retains essential two-dimensional characteristics. There is active research on modeling these flames by solving Navier-Stokes equations. However, even presuming the most optimistic outcomes of such research, incorporating elementary combustion chemistry is a computationally intensive task, even without mist.

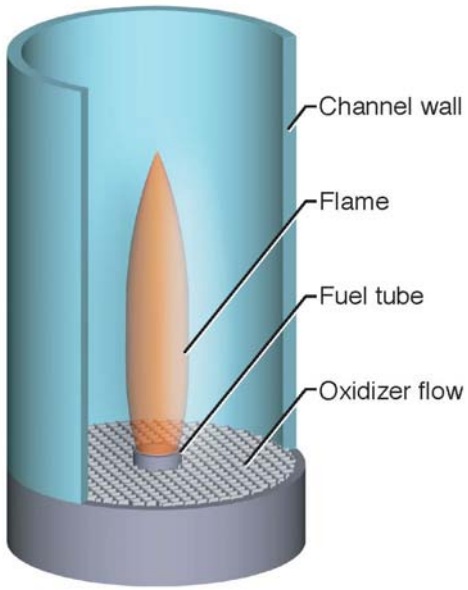

Figure 1: Schematic of the axisymmetric confined coflowing non-premixed flame configuration. As illustrated here the fuel issues through the center tube and the oxidizer velocity profile is flattened by a honeycomb flow straightener.

To model a particle-laden reacting flow, a multicontinua approach as described by Sirignano [9] can be used. Such an approach can be implemented using a Lagrangian/Eulerian technique in which the particle dynamics are handled in a Lagrangian framework and appropriate source terms are incorporated into the Eulerian gas-phase conservation equations. There is mass and energy exchange between the particles and the gas-phase flow, which contribute to source (or sink) terms in the gas-phase conservation equations. Inasmuch as the source terms depend on the particle dynamics and vice versa, iterations are needed. However, this approach is practical only if the computation time needed to model the reacting gas flow is small. Even in geometrically simple configurations, such as co-flowing flames, the computational cost of a full Navier-Stokes solution of the reacting flow alone is prohibitively high.

The objective of the work reported here is to develop and validate computationally efficient models of non-premixed laminar jet flames using boundary-layer approximations. This approach will provide the needed efficiency for the modeling of flame/mist interactions. By no means is the boundary-layer approach a general alternative to full multidimensional modeling. However there are practical circumstances where laboratory flames can be modeled accurately, but using a very small fraction of the computational resources that would be required by a full two-dimensional simulation. Even recognizing some compromise in accuracy, there is enormous utility in developing models that can be exercised frequently and at low cost.

The first quantitative solution to the steady laminar jet flame was published in 1928 by Burke and Schumann [10]. Since then researchers have developed computational models that relax virtually all the assumptions related to the flow dynamics and chemical kinetics. The first models

to incorporate detailed chemistry and transport were developed by Miller and Kee [11, 12]. They used a boundary-layer formulation and a finite-difference marching algorithm, with chemistry handled by an operator-splitting method. Heys et al. [13] modeled Bunsen-like flames in boundary-layer form. They used a von Mises approach to transform the radial coordinate to the streamfunction as an independent variable. They incorporated kinetic-theory representations of the transport properties, but used relatively global chemistry. This model matched measured species and temperature profiles very accurately. Takagi and Xu [14] also used a boundary-layer formulation to model the effects of preferential diffusion in methane-air jet flames. Their solution algorithm was based on Spalding's GENMIX approach [15] and incorporated a 29-step reaction mechanism. The Takagi and Xu model also represented measured profiles accurately.

Smooke et al. [16] were the first to model jet flames by solving the steady-state Navier-Stokes equations as an elliptic problem. Local adaptive mesh refinement provided resolution in the flame zones, with larger meshes elsewhere. Day and Bell [17] modeled the transient low-Mach-number Navier-Stokes equations. This model also implements adaptive mesh refinement to deliver very high resolution in the flame zone. Sullivan et al. [18] and Bell et al. [19] used this model to simulate experiments measuring NOx formation. Katta et al. [20] developed Navier-Stokes models to study transient jet-flame instabilities and traveling vortices at the edges of the flame. The chemically reacting Navier-Stokes models provide solutions that capture accurately full multidimensional complexity. However, they do so at a computational cost running from many hours to many days. Consequently it is impractical to use these models for extensive parameter studies or embed them iteratively into other models.

In this paper we develop and demonstrate a boundary-layer formulation of the co-flow system and a highly efficient solution algorithm. We use specific metrics to evaluate the validity of the boundary-layer formulation as a function of flow conditions. We also present some preliminary results that characterize the one-way coupled interaction of a water mist with that flame.

BOUNDARY-LAYER EQUATIONS

The boundary-layer equations are derived from the Navier-Stokes equations using dimensional scaling arguments to show that the axial diffusion and radial pressure variations can be neglected under certain circumstances. The details of this scaling analysis for reacting channel flow may be found in Kee, et al. [21]. The conservation equations are reduced from essentially elliptic to parabolic, with the time-like independent variable being the distance along the channel. Consequently the system can be solved by an efficient one-pass marching algorithm. No source terms related to the mist are included in the equations below since this paper focuses on the flame solution in the absence of the mist. Only one-way coupled results are briefly discussed at the end of the paper to illustrate the possible extension to multiphase reacting flow. The boundary-layer equations are

$$\frac{\partial(\rho u)}{\partial z} + \frac{1}{r}\frac{\partial(r\rho v)}{\partial r} = 0, \tag{1}$$

$$\rho u\frac{\partial u}{\partial z} + \rho v\frac{\partial u}{\partial r} = -\frac{\partial p}{\partial z} - \rho g + \frac{1}{r}\frac{\partial}{\partial r}\left(r\mu\frac{\partial u}{\partial r}\right), \tag{2}$$

$$\frac{\partial p}{\partial r} = 0, \tag{3}$$

$$\rho u c_p\frac{\partial T}{\partial z} + \rho v c_p\frac{\partial T}{\partial r} = u\frac{\partial p}{\partial z} - u\rho g + \frac{1}{r}\frac{\partial}{\partial r}\left(r\lambda\frac{\partial T}{\partial r}\right) - \sum_{k=1}^{K} c_{pk} j_{r,k}\frac{\partial T}{\partial r} - \sum_{k=1}^{K} h_k\dot{\omega}_k M_k \tag{4}$$

$$\rho u\frac{\partial Y_k}{\partial z} + \rho v\frac{\partial Y_k}{\partial r} = -\frac{1}{r}\left(\frac{\partial r j_{r,k}}{\partial r}\right) + \dot{\omega}_k M_k, \tag{5}$$

$$\rho = \frac{p\overline{M}}{RT}; \qquad \overline{M} = \left(\sum_{k=1}^{K}\frac{Y_k}{M_k}\right)^{-1}, \tag{6}$$

$$j_{r,k} = \rho Y_k V_{kr}; \qquad V_{r,k} = \frac{1}{X_i\overline{M}}\sum_{j\neq k}^{K} M_j D_{kj}\frac{\partial X_j}{\partial r} - \frac{D_k^T}{\rho Y_k}\frac{1}{T}\frac{\partial T}{\partial r}. \tag{7}$$

The independent variables are the spatial coordinates z and r. The dependent variables are the axial and radial velocities u and v, pressure p, temperature T, and the species mass fractions Y_k. The density ρ is determined from the other variables via the equation of state. Thermodynamic and transport variables include the viscosity μ, heat capacity c_p, thermal conductivity λ, ordinary diffusion coefficients D_{jk}, and thermal diffusion coefficients D_k^T. The species enthalpies are h_k and molecular masses are M_k. The molar chemical production rates by homogeneous chemical reaction are represented by $\dot{\omega}_k$. The radial diffusive mass fluxes are $j_{r,k}$ and the radial diffusion velocities are represented as $V_{r,k}$, with X_k being the mole fractions. Gravitational acceleration is represented as g. In the work reported here the CHEMKIN [22, 23] software is used to evaluate properties as well as reaction rates.

The boundary-layer equations have a differential-algebraic equation (DAE) character [24, 25], which must be considered in designing robust computational solution algorithms. Importantly, the radial velocity $v$behaves as an algebraic constraint in the sense that it does not have a time-like (i.e., z) derivative. The pressure gradient dp/dz behaves as a dependent variable that does not have a time-like derivative.

It can be shown that for any radial profiles of $u(r)$, $T(r)$, and $Y_k(r)$ at some z, there is only one possible profile of $v(r)$ that satisfies the continuity equation. Because the radial velocity must vanish at the centerline and the outer channel wall, a further constraint is imposed on the first-order continuity equation. Specifically the pressure gradient dp/dz takes the role of an eigenvalue that is determined to enable satisfaction of the two boundary conditions on v. Despite the fact

that the pressure gradient appears to be a time-like derivative of the dependent variable p, it cannot be used as such. Doing so renders the DAE system to be index 2, which is problematic for most DAE solution software such as DASSL [24] or LIMEX [26].

Initial Conditions

At the entrance (z=0) $u(r)$, $T(r)$, and $Y_k(r)$ profiles may be specified somewhat arbitrarily. However, consider the particular situation for a central jet of fuel issuing into a co-flowing oxidizer stream. The velocity profiles in the central tube and the annular co-flow region may be determined from exact solutions to the fully developed pipe-flow problems. Alternatively, flat velocity profiles may be established using honeycombs of porous manifolds (e.g., Fig. 1). The temperature profile may be taken as uniform in the two streams. The species composition in the central tube represents the fuel with the annular region carrying the oxidizer.

There is a finite region in which the fuel and oxidizer mix, usually related to the tube-wall thickness. The inlet profiles must be such that a flame will be established and propagate. Using the specified profiles, the constrained enthalpy-pressure chemical equilibrium may be evaluated within the mixing region to provide self-consistent temperature and species profiles. Although any $u(r)$, $T(r)$, and $Y_k(r)$ profiles may be specified, the $v(r)$ profiles are not arbitrary. In fact they must be constrained to satisfy the continuity equation. Failing to satisfy this constraint will cause error-controlled DAE software to fail as a result of inconsistent initial conditions.

Boundary Conditions

The boundary conditions for the momentum, energy, and species equations are:

$$\text{at } r = 0 : \frac{\partial u}{\partial r} = 0, \quad \frac{\partial T}{\partial r} = 0, \quad \frac{\partial Y_k}{\partial r} = 0. \tag{8}$$

$$\text{at } r = R : u = 0, \quad T = T_w(z), \quad \rho Y_k V_k = 0. \tag{9}$$

The remaining boundary condition is for the radial velocity v, which vanishes at both the centerline and the channel wall.

Physical Limitations

Although the initial-condition specification described above is sufficient mathematically, the physical stabilization mechanism for non-premixed jet flames depends on axial diffusion in the burner region. Since the boundary-layer equations specifically exclude axial diffusion, the physical basis for flame stabilization cannot be represented and the solutions must be regarded as approximate in the near-nozzle region. Nevertheless, once downstream of the stabilization region the flame structure predicted by boundary-layer models can be very accurate.

Most laboratory flames are relatively low speed and buoyancy dominated. The natural flame diameter depends primarily on the fuel flow rate and only weakly on the nozzle diameter. Since

the flame diameter persists over much of the flame length, it is advisable to make the nozzle diameter comparable to the flame diameter. If the nozzle diameter is much different then the flame must adjust rapidly to its natural position, causing inaccuracies and computational difficulties in the near-nozzle region as the flame zone moves laterally [11, 12].

Partially premixed streams can also be the source of inaccuracies and computational difficulties. For example if the fuel jet contains a flammable fuel-oxidizer mixture then the ignition and stabilization process depends on axial diffusive transport. Again, any prediction and interpretation of the premixed flame structure and flame position in the near-nozzle region must be viewed with great caution.

As the flow velocities increase the scaling arguments show that the boundary-layer approximations improve. However, at sufficiently high velocities the flow can become unstable [20, 27]. At first there may be wave-like wrinkling of the flame, ultimately transitioning to turbulent flow. Under these circumstances any steady-flow analysis must break down. Fortunately, for confined co-flow flames such as those described by Sullivan, et al. [18] the laboratory flames are observed to remain stable to relatively high flow rates.

Solution Algorithm

A method-of-lines approach is used to solve the semi-discrete system, which is a system of DAEs. The radial mesh spans the domain between the centerline and the outer channel wall. The radial mesh spacing may be nonuniform, but it remains fixed throughout the channel. The marching solution is accomplished with DASSL, which implements an implicit, variable-order, variable-stepsize method based on the backward differentiation formula (BDF) method [24].

NOMINAL FLAME

Figure 2 illustrates the computed solution to a representative flame. The geometry and flow conditions are taken to represent the flame reported by Sullivan, et al. [18]. The inner radii of the fuel and the oxidizer tube are 6 mm and 14 mm, respectively. The outer radius of the fuel tube is 7 mm. The channel-wall temperature rises linearly from 500 K at the inlet to 800 K at z=6cm, then drops linearly to 300 K at z=50cm. The fuel is a mixture of methane and nitrogen (150 cm^3/min of CH_4 and 220 cm^3/min of N_2) and the co-axial stream is air (840 cm^3/min of $O_2$and 3160 cm^3/min of N_2). Both streams are initially 300 K. At the initial condition the fuel velocity profile is parabolic and the velocity profile in the annular air stream is the quadradic solution to the laminar-annular-channel problem. Peak velocities in the fuel and air streams are 12 cm/s and 22 cm/s, respectively.

The inlet mixing zone is centered at half the thickness of the fuel nozzle (r=6.5mm) and the width of the mixing zone is set to 4 mm. After computing the air profile from the fuel profile, an enthalpy-pressure equilibrium is computed for each mesh point within the mixing zone. This produces new temperature and species profiles. The axial velocity in the mixing zone is taken as a Gaussian with a peak at the location of the peak temperature. In this case the peak axial velocity in the mixing zone is u=50cm/s. The solutions shown in Fig. 2 were computed using

GRI-Mech 3.0 [28], but with the nitrogen-cycle chemistry neglected. A uniform radial mesh of 43was used in the results shown.

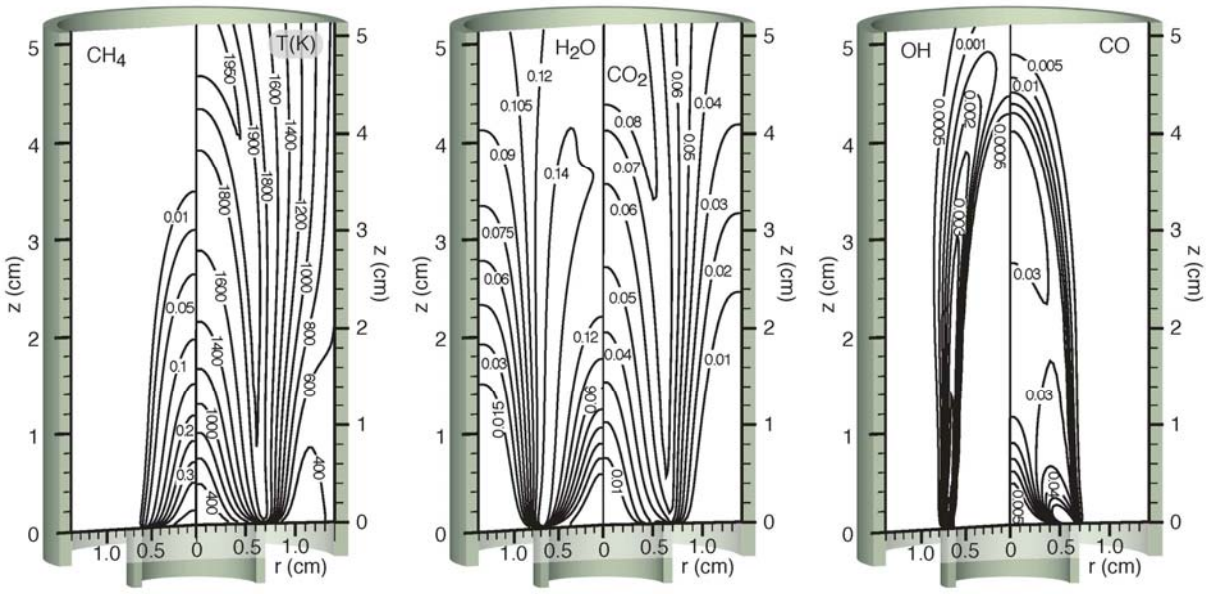

Figure 2: Contour maps of selected solution components for the nominal problem. The species contours represent the mole fractions.

The boundary-layer solutions are generally quite similar to those reported by Sullivan, et al. [18], but there are significant differences. The flame length predicted here is approximately 4.9cm with a maximum temperature of 1970 K (The adiabatic flame temperature for is 2080 K). Based on the Navier-Stokes simulation, Sullivan reports a flame length of approximately 3.6cm and a maximum flame temperature of 1847 K. We find that the flame length is sensitive to the specified inlet conditions. Bell et al. [19] also report that the Navier-Stokes simulations show that flame length is sensitive to inlet boundary conditions. Fortunately, away from the inlet region the flame structure itself is not too sensitive to the inlet conditions. Regardless of the model used, it is clear that establishing inlet conditions is important to model-based experimental interpretation.

Explaining the different maximum temperatures between the Navier-Stokes model reported by Sullivan et al. [18] and the boundary-layer model remains elusive. Since flame temperature depends on radical-recombination chemistry it is important to model accurately the transport and reaction of species like H. By increasing the number of mesh points in the boundary-layer model, the flame temperature is found to be insensitive to mesh resolution. This indicates that convective and diffusive transport is being handled accurately. Switching between the GRI mechanism and a reduced C1 mechanism causes only a small change in flame temperature. Thus details of the reaction mechanism are not expected to be causing different temperature predictions. Including axial diffusion would tend to reduce radical concentrations in the flame zone, which in turn would tend to reduce flame temperatures. However, based on boundary-layer scaling arguments, this is expected to be a small effect. Since the solutions are clearly sensitive to the inlet boundary conditions and the boundary-condition specifications in the two

formulations are not identical, it is possible that the two formulations are actually solving slightly different problems.

We have also modeled the flame conditions published by Takagi and Xu [14] and our simulations are essentially identical their published results. These results are also in very good agreement with the reported measurements.

Neglected Axial Diffusion

The theoretical basis for neglecting axial diffusion is grounded in an analysis of the nondimensional transport equations and nondimensional parameter groups that characterize the geometry and flow conditions [21, 29]. The scaling arguments show that while axial and radial convection remain order-one, the axial diffusion is small compared to the radial diffusion. In the case of the energy equation this means that

$$\frac{\partial}{\partial z}\left(\lambda\frac{\partial T}{\partial z}\right) \ll \frac{1}{r}\frac{\partial}{\partial r}\left(r\lambda\frac{\partial T}{\partial r}\right). \qquad (10)$$

Since the boundary-layer scaling arguments are general, it is interesting to evaluate quantitatively the magnitude of the neglected term in a particular flame.

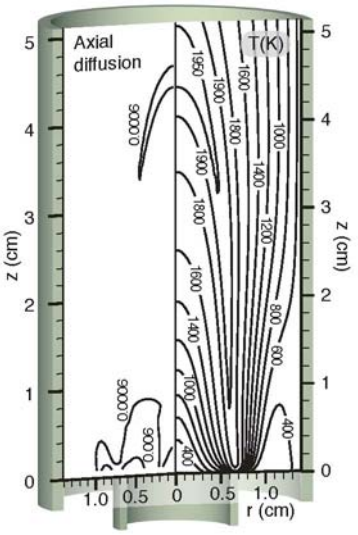

Figure 3: Isotherms and axial-transport map for a methane-air non-premixed flame. This flame is similar to the one shown in Fig. 2. However, it is modeled with a smaller C1 reaction mechanism. The channel-wall boundary is fixed at T_w=500K instead of a specified axial temperature profile. The left-hand panel shows contours of $A(z,r)$ as defined by Eq. 11.

With a solution in hand, such as illustrated in Fig. 3, the axial diffusion can be estimated. The boundary-layer solution provides a two-dimensional field of velocities, temperatures, and composition. From these fields one can evaluate the axial derivatives. As a practical matter, however, numerical differentiation is troublesome. The axial marching solution only controls local truncation error in the dependent variables themselves, not in the higher derivatives. Although the solutions are accurate and smooth, forming finite differences to evaluate second axial derivatives produces results that are too noisy. Therefore it is necessary to smooth the finite-difference evaluation of the first derivative before evaluating the second derivative. The needed smoothing is accomplished with cubic splines using the CUBGCV software [30, 31].

The left-hand panel of Fig. 3 shows contours of a normalized estimate of the axial diffusive transport,

$$A(z,r) = \left\{ \left| \frac{\partial}{\partial z} \left(\lambda \frac{\partial T}{\partial z} \right) \right| \right\} \left\{ \max_{z>0.25} \left[\left| \frac{1}{r} \frac{\partial}{\partial r} \left(r\lambda \frac{\partial T}{\partial r} \right) \right| \right] \right\}^{-1}. \quad (11)$$

The denominator is the maximum magnitude of the radial diffusion above z=0.25cm, which discounts the relatively high diffusion terms in the near-nozzle region. Although the choice of normalization is somewhat arbitrary, the map shows clearly that axial transport is very small and concentrated in the near-nozzle and flame-tip regions. Thus the effects of the neglected term is small and the boundary-layer approximations are very good.

Computational Performance

The solution to the nominal problem was computed in approximately 15 minutes on a 3 GHz personal computer. The solutions show that there is very little chemical activity among the C2 species and trivially small concentrations of higher hydrocarbons. Consequently the flame was again simulated with a reduced C1 mechanism that eliminates species with two or more carbons. The C1 mechanism consists of 58 reactions among 17 species. Additionally the channel-wall boundary condition is fixed at T_w=500K. The reduced simulation (Fig. 3) required only about one minute on a 3 GHz personal computer.

With a method-of-lines solution, the axial meshing is adjusted automatically to maintain stability and assure a certain level of local truncation error. Generally speaking the axial meshing is very fine near the inlet and increases downstream. It is also finer near the flame tip where the solution varies rapidly in the axial direction. The solutions illustrated here use 43 uniform radial meshes (Δr=0.33mm). Mesh-resolution studies with up to 140 uniformly distributed points produce essentially identical solutions. Sullivan et al. [18] reported that their adaptive-mesh-refinement algorithm used local mesh sizes as small as Δr=0.065mm.

The statistics from DASSL reveal some measures of the simulation's performance. For the C1-mechanism solution illustrated in Fig. 3, DASSL took 189 steps up to z=5.2cm. In that interval there were 292 calls to the function (forming the discrete representation of the conservation equations) and 90 Jacobian evaluations. There were 20 error-test failures and 4 convergence-test failures. These statistics indicate very good performance.

INTERACTION OF A POLYDISPERSED MIST WITH THE NOMINAL FLAME

The primary benefit of the fast modeling capability is a significant improvement in computational efficiency without substantially affecting accuracy. Beyond the obvious consequence on parametric studies, this model enables the development of computationally efficient, fully coupled, multiphase flow models. In this section, an existing mist model is used to predict the behavior of a water mist as it interacts in a one-way coupled manner with the flame calculated and discussed above. The details of the mist model are presented in [32, 33] and are only briefly outlined here for completeness.

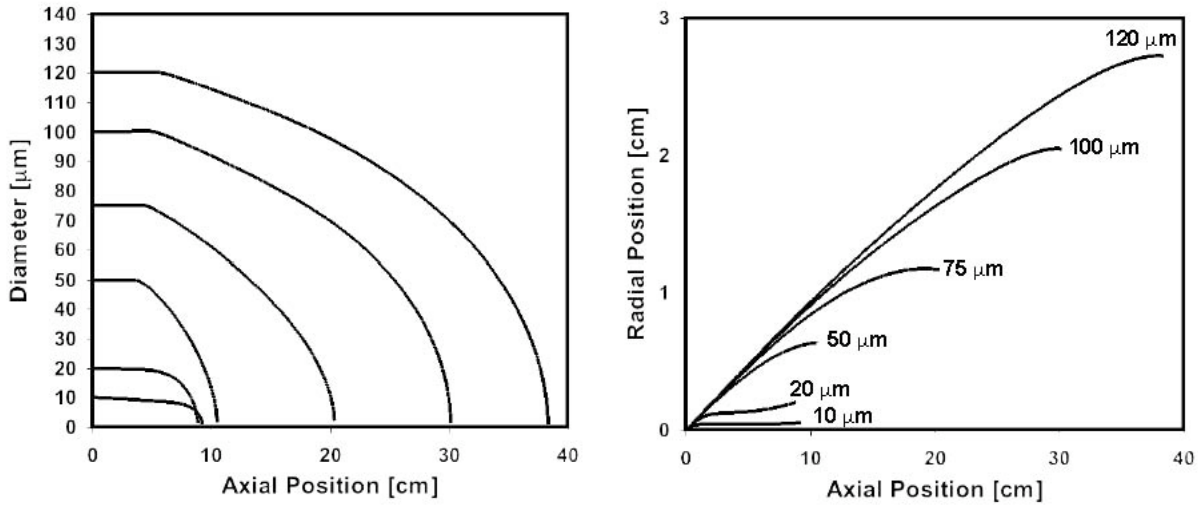

Figure 4: Diameter and trajectories of representative droplets interacting with the nominal flame.

The polydispersed mist is described in a Lagrangian manner that is consistent with the Lagrangian/Eulerian formulation that would be required in two-way coupled simulations. The various distributions characterizing the mist (size, velocity, direction) are discretized stochastically, which further enhances computational efficiency. Representative droplets are defined using a Monte Carlo approach. The dynamic and evaporation behavior of each droplet over the pre-calculated flame is evaluated and each history can be used to reconstruct the mist. The evaporation of each droplet is modeled using an extended film model [33, 34].

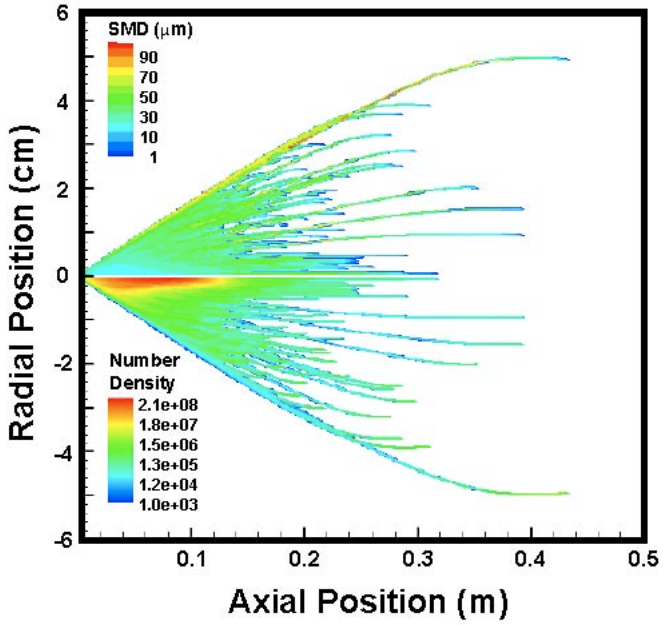

Figure 5: Predicted spatial distribution, sauter mean diameter, and number density of a water mist interacting with the nominal flame.

The predicted behavior of representative droplets with initial diameters from 10 to 120 μm injected at 15 m/s and 290 K in the central fuel stream with a 5^{o}angle is shown in Figure 4. Clearly, the velocity of the smaller droplets (under 20 μm) quickly matches that of the surrounding gas while larger droplets, with more inertia, are more likely to disperse. Expectedly, the droplets do not experience significant evaporation until they are exposed to the larger temperatures associated with the flame. The overall behavior of a mist injected at 300 K with a mean velocity of 15 m/s, a mean diameter of 30 μm, a full cone angle of 30^{o}, and m=100g/s is shown in Figure 5. While the smaller droplets disappear within the flame region, the lifetime of larger droplets extends largely beyond that region, up to 40 cm axially for the 120 μm drops. This indicates that such large droplets would be inefficient in contributing to the extinction of the flame.

CONCLUSIONS

A highly efficient algorithm has been developed to model coaxial nonpremixed flames in a boundary layer form. The approach is based on a method-of-lines solution to a semi-discrete representation of the conservation equations, forming a system of differential-algebraic equations. By retaining the physical coordinates as the independent variables (instead of a von Mises transformation) the mesh points tend to remain within the flame zone. Because the boundary-layer approximations are found to be valid for many laboratory flame experiments, the approach provides an enabling tool to analyze and interpret experimental observations on detailed flame structure. Moreover, the computational efficiency of the algorithm enables its incorporation into iterative algorithms to simulate reactive multiphase flow relevant to water-mist fire suppression issues.

ACKNOWLEDGMENT

This material is based upon work supported by the National Aeronautics and Space Administration, under Grant NNC04AA13A, Dr. Suleyman Gokoglu, Technical Monitor (NASA Glenn Research Center, Cleveland, OH) and through the Center for the Commercial Applications of Combustion in Space (CCACS) at the Colorado School of Mines. We are grateful to Drs. Joe Grcar, Marc Day, and John Bell (LBNL) for sharing and discussing details of their Navier-Stokes flame simulations.

REFERENCES

[1] K.Prasad, G.Patnaik, and K.Kailasanath. A numerical study of water-mist suppression of large scale compartment fires. *Fire Safety Journal*, 37 (2002) 569-589.

[2] G.Back, III, G.Beyler, and R.Hansen. A quasi-steady state model for predicting fire suppression in spaces protected by water mist systems. *Fire Safety Journal*, 35 (2000) 327-362.

[3] R.Wighus and A.W. Brandt. Watmista one-zone model for water mist fire suppression. *Halon Options Technical Working Conference*, (2001) 111–121.

[4] A.Abbud-Madrid, S.J. Lewis, J.D. Watson, J.T. McKinnon, and J.-P. Delplanque. Study of water mist suppression of electrical fires for spacecraft applications: Normal gravity results. *Proceedings of the Halon Options Technical Working Conference, HOTWC 2005. May 24-26, 2005, Albuquerque, NM*.

[5] A.M. Lentati and H.K. Chelliah. Dynamics of water droplets in a counterflow field and their effect on flame extinction. *Combustion and Flame*, 115 (1998) 158-179.

[6] S.P. Fuss, E.F. Chen, W.Yang, R.J. Kee, B.A. Williams, and J.W. Fleming. Inhibition of premixed methane/air flames by water mist. *Proccedings of the Combustion Institute*, 29 (2002) 361-367.

[7] W.Yang and R.J. Kee. The effect of monodispersed water mists on the structure, burning velocity, and extinction behavior of freely propagating, stoichiometric, premixed, methane-air flames. *Combustion and Flame*, 130(2002) 322-336.

[8] W.Yang, T.Parker, H.D. Ladouceur, and R.J. Kee. The interaction of thermal radiation and water mist in fire suppression. *Fire Safety Journal*, 39 (2004) 41-67.

[9] W. A. Sirignano, *Fluid Dynamics and Transport of Droplets and Sprays*. Cambridge University Press, 1999.

[10] S. P. Burke, T. E. W. Schumann, Diffusion flames. *Ind. Engin. Chem.* 20 (1928) 998–1004.

[11] J. A. Miller, R. J. Kee, Chemical Nonequilibrium Effects in Hydrogen-Air Laminar Jet Diffusion Flames. *J. Phys. Chem.* 81 (1977) 2534–2542.

[12] R. J. Kee, J. A. Miller, A Split-Operator, Finite-Difference Solution for Axisymmetric Laminar-Jet Diffusion Flames. *AIAA J.* 16 (1978) 169–176.

[13] N.W. Heys, F.G. Roper, P.J. Kayes, A Mathematical Model of Laminar Axisymmetric Natural Gas Flames. *Computers and Fluids* 9 (1981) 85–103.

[14] T. Takagi, Z. Xu, Numerical Analysis of Laminar Diffusion Flames–Effects of Preferential Diffusion of Heat and Species. *Combust. Flame* 96 (1994) 50–59.

[15] D.B. Spalding, *HMT Genmix–A General Computer Program for Two-Dimensional Parabolic Phenomena*. Pergamon, New York, 1977.

[16] M.D. Smooke, R.E. Mitchell, D.E. Keyes, Numerical Solution of Two-Dimensional Laminar Diffusion Flames. *Combust. Sci. Techn.* 67 (1989) 85–122.

[17] M.S. Day, J.B. Bell, Numerical Simulation of Laminar Reacting Flows with Complex Chemistry. *Combust. Theory and Modeling* 4 (2000) 535–556.

[18] N. Sullivan, A. Jensen, P. Glarborg, M. Day, J. Grcar, J. Bell, C. Pope, R.J. Kee, NOx Formation and Ammonia Conversion in Laminar Coflowing Nonpremixed Methane-Air Flames. *Combust. Flame* 131 (2002) 285–298.

[19] J.B. Bell, M.S. Day, J.F. Grcar, W.G. Bessler, C. Schulz, P. Glarborg, A.D. Jensen, Detailed Modeling and Laser-Induced Fluorescence Imaging of Nitric Oxide in a NH_3-Seeded Non-Premixed Methane/Air Flame. *Proc. Combust. Inst.* 29 (2002) 2195–2202.

[20] V.R. Katta, L.P. Goss, W.M. Roquemore, Effect of Nonunity Lewis Number and Finite-

Rate Chemistry on the Dynamics of a Hydrogen-Air Jet Diffusion Flame. *Combust. Flame* 96 (1994) 60–74.

[21] R.J. Kee, M.E. Coltrin, P. Glarborg, *Chemically Reacting Flow: Theory and Practice*. John Wiley, New York, 2003.

[22] R.J. Kee, F.M. Rupley, E. Meeks, J. A. Miller, *Chemkin-III: A Fortran Chemical Kinetics Package for the Analysis of Gas-Phase Chemical and Plasma Kinetics*. Technical Report SAND96-8216, Sandia National Laboratories, 1996.

[23] R. J. Kee, G. Dixon-Lewis, J. Warnatz, M. E. Coltrin, J. A. Miller, *A Fortran Computer Code Package for the Evaluation of Gas-Phase Multicomponent Transport Properties*. Technical Report SAND86-8246, Sandia National Laboratories, 1986.

[24] K.E. Brenan, S.L. Campbell, L.R. Petzold, *Numerical Solution of Initial-Value Problems in Differential Algebraic Equations*. SIAM, Philadelphia, PA, second edition, 1996.

[25] U.M. Ascher, L.R. Petzold, *Computer Methods for Ordinary Differential Equations and Differential-Algebraic Equations*. SIAM, Philadelphia, PA, 1998.

[26] P. Deuflhardt, E. Hairer, J. Zugk, One-Step and Extrapolation Methods for Differential Algebraic Systems. *Num. Math.* 51 (1987) 501–516.

[27] H. Yamashita, G. Kushida, T. Takeno, A Numerical Study of the Transition of Jet Diffusion Flames. *Proc. R. Soc. Lond. A* 431 (1990) 301–314.

[28] G.P. Smith, D.M. Golden, M. Frenklach, N.W. Moriarty, B. Eiteneer, M. Goldenberg, C.T. Bowman, R.K. Hanson, S. Song, W.C. Gardiner, V. Lissianski, Z. Qin, *GRI-Mech—An Optimized Detailed Chemical Reaction Mechanism for Methane Combustion*. Technical Report http://www.me.berkeley.edu/gri mech, Gas Research Institute, 1999.

[29] S. H. Chung, C. K. Law, Burke-Schumann Flame with Streamwise and Preferential Diffusion. *Combust. Sci. Techn.* 37 (1984) 21–46.

[30] M.F. Hutchinson, F.R. deHoog, Smoothing Noisy Data with Spline Functions. *Numer. Math.* 4 (1986) 99–106.

[31] M.F. Hutchinson, Algorithm 642: A Fast Procedure for Calculating Minimum Cross-Validating Cubic Smoothing Splines. *ACM Trans. Math. Software* 12 (1986) 150–153.

[32] S.B. Johnson, S.J. Lewis, and J.-P. Delplanque. Droplet-resolved dilute spray evaporation model, (HT-FED2004-56898) *Heat Transfer/Fluids Engineering Summer Conference*, Charlotte, North Carolina, USA, July 2004.

[33] S.J. Lewis, J.-P. Delplanque, A.Modak, and R.Kee. Behavior of polydispersed water mist in reacting flow fields. *Spring meeting of the Western States Sections of the Combustion Institute*, Davis, CA, 2004.

[34] B.Abramzon and W.A. Sirignano. Droplet vaporization model for spray combustion calculations. *International Journal of Heat and Mass Transfer*, 32 (1989) 16051618.